



Air–sea exchange of CO₂ at a Northern California coastal site along the California Current upwelling system

H. Ikawa^{1,2,4}, I. Faloona², J. Kochendorfer^{2,3}, K. T. Paw U², and W. C. Oechel¹

¹Global Change Research Group, San Diego State University, 5500 Campanile Dr., San Diego, CA 92182-4614, USA

²Department of Land, Air, and Water Resources, University of California Davis, One Shield Ave, Davis, CA 95616 8627, USA

³Atmospheric Turbulence and Diffusion Division, NOAA, 456 S. Illinois Ave., Oak Ridge, TN 37830, USA

⁴International Arctic Research Center, University of Alaska, Fairbanks, 930 Koyukuk Dr., P.O. Box 757340, Fairbanks, AK 99775-7340, USA

Correspondence to: H. Ikawa (hikawa.biomet@gmail.com)

Received: 23 October 2012 – Published in Biogeosciences Discuss.: 12 December 2012

Revised: 25 May 2013 – Accepted: 31 May 2013 – Published: 1 July 2013

Abstract. It is not well understood whether coastal upwelling is a net CO₂ source to the atmosphere or a net CO₂ sink to the ocean due to high temporal variability of air–sea CO₂ exchange (CO₂ flux) in coastal upwelling zones. Upwelling transports heterotrophic, CO₂ enriched water to the surface and releases CO₂ to the atmosphere, whereas the presence of nutrient-rich water at the surface supports high primary production and atmospheric CO₂ uptake. To quantify the effects of upwelling on CO₂ flux, we measured CO₂ flux at a coastal upwelling site off of Bodega Bay, California, with the eddy covariance technique during the summer of 2007 and the fall of 2008, and the bulk method with partial pressure of CO₂ of surface water (*p*CO₂) data from November 2010 to July 2011. Variations in sea surface temperatures (SST) and alongshore wind velocity suggest that the measurement period in 2007 coincided with a typical early summer upwelling period and the measurement period in 2008 was during a typical fall relaxation period. A strong source of CO₂ ($\sim 1.5 \pm 7$ SD (standard deviation) g C m⁻² day⁻¹) from the ocean to the atmosphere during the upwelling period was concurrent with high salinity, low SST, and low chlorophyll density. In contrast, a weak source of CO₂ flux ($\sim 0.2 \pm 3$ SD g C m⁻² day⁻¹) was observed with low salinity, high SST and high chlorophyll density during the relaxation period. Similarly, the sink and source balance of CO₂ flux was highly related to salinity and SST during the *p*CO₂ measurement periods; high salinity and low SST corresponded to high *p*CO₂, and vice versa. We estimated that

the coastal area off Bodega Bay was likely an overall source of CO₂ to the atmosphere based on the following conclusions: (1) the overall CO₂ flux estimated from both eddy covariance and *p*CO₂ measurements showed a source of CO₂; (2) although the relaxation period during the 2008 measurements were favorable to CO₂ uptake, CO₂ flux during this period was still a slight source; (3) salinity and SST were found to be good predictors of the CO₂ flux for both eddy covariance and *p*CO₂ measurements, and 99 % of the historical SST and salinity data available between 1988 and 2011 fell within the range of our observations in May–June 2007, August–September 2008 and November 2010–July 2011, which indicates that our data set was representative of the annual variations in the sea state. Based on the developed relationship between *p*CO₂, SST and salinity, the study area between 1988 and 2011 was estimated to be an annual source of CO₂ of ~ 35 mol C m⁻² yr⁻¹. The peak monthly CO₂ flux of ~ 7 mol C m⁻² month⁻¹ accounted for almost 30 % of the dissolved inorganic carbon in the surface mixed layer.

1 Introduction

Intensive efforts have been underway over the last few decades to better understand and quantify global air–sea CO₂ exchange. These investigations reveal that the oceans absorb approximately one-third of the global anthropogenic CO₂ emissions (Gruber et al., 2009; Takahashi et al., 2009), and

have accumulated 118 (± 19) Pg C of carbon emitted by fossil fuel combustion, land use change, and cement production between 1800 and 1994 (Sabine et al., 2004). However, current estimates of the global ocean CO₂ uptake still contain considerable uncertainty, and more observations are necessary to better understand this critical carbon reservoir (Doney et al., 2009). One of the largest uncertainties in the global carbon cycle is the role of coastal seas, which potentially account for 30 % of the net global sink of CO₂ from the atmosphere to the ocean (Chen and Borges, 2009). Current global estimates do not account for the variability of the coastal ocean due to the difficulties of quantifying coastal CO₂ fluxes (Takahashi et al., 2009). In order to better understand the dynamics of coastal CO₂ fluxes, we must understand the physical and biological processes unique to coastal waters that control these fluxes.

Coastal upwelling is an important process that conflates the physical and biological influences on the coastal carbon cycle (Dugdale et al., 2006; Gattuso et al., 1998). Upwelling conveys deep nutrient-rich water to the surface and supports diverse coastal ecosystems. Although the surface of coastal upwelling zones covers only 1 % of the global ocean, these areas support approximately 50 % of the fishery industry because of their high primary productivity (Gattuso et al., 1998). Observational studies indicate that upwelling along the California coast has increased over the past 30 yr (Garcia-Reyes and Largier, 2010). This intensification of upwelling is likely related to increasing greenhouse gases, as the increasing temperature difference between land and sea accelerates coastal upwelling (Bakun, 1990; Diffenbaugh et al., 2004).

The sign of the effects of coastal upwelling on CO₂ fluxes has been debated. Upwelling provides a source of CO₂ from the ocean to the atmosphere because deep water is enriched with respired CO₂. At the same time, upwelling carries nutrients to the surface that enhance the biological uptake of CO₂ (Borges and Frankignoulle, 2002). Thus the net CO₂ flux in upwelling zones averaged for inter-seasonal scales can be a sink of CO₂ from the atmosphere to the ocean (Evans et al., 2011; Gago et al., 2003; Hales et al., 2005; Ianson and Allen, 2002). The source and sink pulses of CO₂ flux reported in past studies range from -10 to $+30$ mol C m⁻² yr⁻¹ (Copin-Montegut and Raimbault, 1994; Friederich et al., 2002; Goyet et al., 1998; Hales et al., 2005; Ianson and Allen, 2002; Ianson et al., 2009; Kelley and Hood, 1971; Lendt et al., 2003; Simpson and Zirino, 1980; Torres et al., 1999), using the sign convention of positive fluxes into the atmosphere from the ocean, and they are frequently two orders of magnitude greater than the global average net CO₂ flux of approximately -0.4 mol C m⁻² yr⁻¹ (Takahashi et al., 2009). This emphasizes the importance of understanding CO₂ fluxes in the complex coastal zones where upwelling occurs. Despite its importance, uncertainty in determining the net CO₂ flux in upwelling zones remains due to the spatial and temporal sparsity of the available measurements.

Another uncertainty in the CO₂ flux of coastal upwelling zones is attributed to the fact that a standard measurement technique for air–sea CO₂ flux is still under development. Quantifications of the spatial and temporal variations of CO₂ flux in upwelling zones were made, for example, by Friederich et al. (2002) for the California coast and Evans et al. (2011) for the Oregon coast. However, these past studies estimated the CO₂ flux using the bulk method based on the partial pressure of CO₂ ($p\text{CO}_2$) measured in surface waters. Currently, the gas transfer velocity required for the bulk method is determined solely by empirical relationships between gas transfer velocity and wind speed, which were developed in the open ocean where wind speeds are generally much higher than coastal areas (Ho et al., 2006; Wanninkhof and McGillis, 1999). Under lower wind speeds, the effects of factors such as surface films and rain may be important as well for determining gas transfer properties (Frew et al., 2004; Jähne et al., 1987), and the effects of breaking waves and bubbles may be especially influential in coastal seas (Keeling, 1993).

The eddy covariance technique utilized in this study is considered to be the most direct CO₂ flux measurement method available. The application of the technique to ocean fluxes is still challenging due to the fact that data processing introduces high uncertainty to the measurement of smaller fluxes (less than 1 g C m⁻² day⁻¹) and the sensors are sensitive to contamination in marine environments (Else et al., 2011; Iwata et al., 2005; Prytherch et al., 2010). However, frequent maintenance and the expected large magnitude of the CO₂ fluxes from coastal upwelling zones enabled us to employ the open path eddy covariance technique.

The objective of this study was to quantify the CO₂ flux from the wind-driven upwelling zone near Bodega Bay, California, and evaluate the physical and biological effects of upwelling on the observed near-shore CO₂ flux. We hypothesized that the sink or source characteristics of the coastal region are reflected in environmental signals that are sensitive to the transports of CO₂ enriched water to the surface and primary productivity. To test this hypothesis, we measured CO₂ fluxes using the eddy covariance technique and the bulk transfer method with $p\text{CO}_2$ measurements and compared the observed CO₂ fluxes with environmental variables related to upwelling events (e.g., wind speed, salinity, sea temperature) and primary production (e.g., light and nutrient availability and chlorophyll density).

2 Methods

2.1 Site descriptions

The study site was located at the intertidal zone in the vicinity of the University of California Davis Bodega Bay Marine Laboratory (BML) in northern California (Fig. 1). The coastal sea of northern California is classically characterized

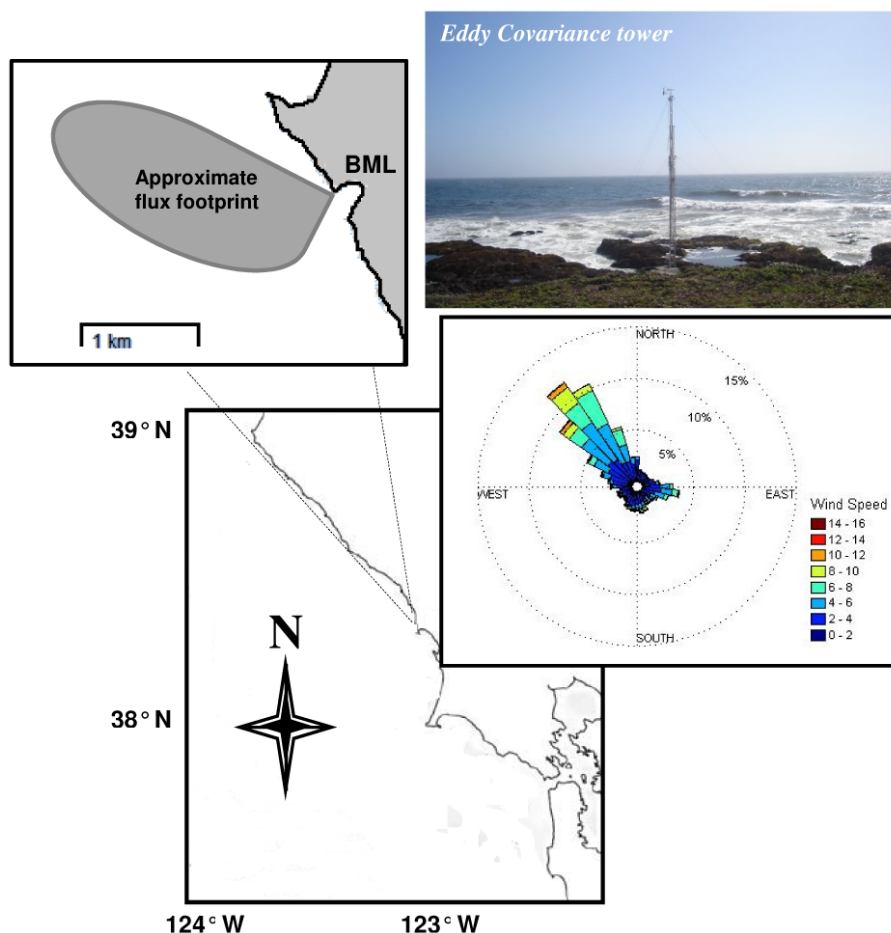


Fig. 1. Study site with the approximate 90 % flux footprint, and the wind rose of daily averaged wind direction and speed (1990–2008) in Bodega Bay, California ($38^{\circ}18'58''$ N, $123^{\circ}04'20''$ W).

by northerly winds in the summer due to the lateral pressure gradient (Dorman et al., 2000) established by the Pacific High offshore. The predominant alongshore wind causes Ekman transport along with lateral shear vorticity, which generates positive curl in the surface stress, resulting in strong coastal upwelling. Spatial distributions of water temperature indicated that our study area was particularly favorable for wind-driven upwelling events (Day and Faloon, 2009). The region's wind-driven upwelling cycle, nutrient availability and subsequent primary production have been described in CoOP WEST (Wind Events and Shelf Transport) studies (Dugdale et al., 2006; Largier et al., 2006; Wilkerson et al., 2006). The region's typically strong winds are periodically interrupted by a period with weaker winds known as a relaxation period, which lasts for ~ 3 –7 days. The repeating cycles of upwelling and relaxation create a unique biological system. Upwelling carries deep water that is relatively cold and nutrient rich to the surface, but increased turbidity (Day and Faloon, 2009) and lateral exports of nutrients inhibit production, while nutrients brought up to the surface are

consumed during the subsequent relaxation period (Largier et al., 2006; Wilkerson et al., 2006).

The eddy covariance measurement period of 2007 and 2008 coincided with a neutral period in the El Niño–Southern Oscillation. The winter of 2010, when $p\text{CO}_2$ measurements were operated, was subject to moderate El Niño conditions.

2.2 Eddy covariance measurements

2.2.1 Data collection

Eddy covariance CO₂ flux measurements were recorded from 28 May to 5 June in 2007 and from 31 August to 25 September in 2008. A three-dimensional sonic anemometer (C-SAT3, Campbell Scientific, USA) and an open path infrared gas analyzer (ATDD, NOAA, USA in 2007 (Auble and Meyers, 1992) and LI-7500, LI-COR Biogeosciences, USA in 2008) were mounted on a 13 m tower within an intertidal zone ($38^{\circ}18'58''$ N, $123^{\circ}04'20''$ W). The density of CO₂ and H₂O, three-dimensional wind components, and sonic temperature were recorded at 10 Hz. The data were stored in a

compact flash memory card in a datalogger (CR1000; Campbell Scientific, USA) and manually collected.

2.2.2 CO₂ flux calculations

Mixing ratios of CO₂ and H₂O to dry air were computed for each 10 Hz data point based on the ideal gas law; air temperature at each 10 Hz data point was computed from the sonic temperature and the vapor pressure calculated from the H₂O density, and the dry air pressure at each 10 Hz data point was computed from the vapor pressure and atmospheric pressure. High frequency data were not available for atmospheric pressure, so standard atmospheric pressure was used. Downward winds possibly increase static pressure, which results in a non-negligible increase of the cumulative CO₂ flux in the long term (Zhang et al., 2011). However, the pressure effect is generally very small ($\sim 3\%$ in Nakai et al., 2011), and we assumed that the effect is negligible in the short-term measurements presented here.

Each 10 Hz measurement of the mixing ratios of CO₂ and H₂O, 3-D wind velocity, and sonic temperature were filtered by a de-spiking algorithm to remove outliers when a datum was greater or less than the median of the 20 adjacent data points ± 6 times their standard deviation (Burba and Anderson, 2010; Vickers and Mahrt, 1997). About 0.02 % of the 10 Hz data points were filtered out and interpolated.

The data stream was divided into 30 min intervals, with the validity of the 30 min averaging period tested using an Ogive function (Foken and Wichura, 1996). The first and second axis-rotation schemes were applied on the three-dimensional wind speeds (Tanner and Thurtell, 1969) for each 30 min data set. The first axis rotation calculates a wind vector along a mean wind direction, and the second axis rotation computes 3-D wind vectors to align the mean vertical wind speed to zero. After the axis rotation, the time lag between the infrared gas analyzer and the sonic anemometer was estimated individually for every 30 min period. Within a -2.0 to $+2.0$ s range, the lag was chosen to maximize the covariance between the CO₂ mixing ratio and the vertical wind speed. On average, the CO₂ mixing ratio measurement had to be advanced by 0.6 s to maximize the correlation with the vertical wind speed measurement. The CO₂ flux was calculated as the covariance between the CO₂ mixing ratio and the vertical wind speed every 30 min (Webb et al., 1980).

2.2.3 Corrections

The effects of the sensor-heating correction (Burba et al., 2008) and cross-sensitivity correction were evaluated. Since the temperature of the infrared gas analyzer detector cell is maintained above the ambient temperature and radiant heating can also increase the temperature of the sensor, the surface of the analyzer can be warmer than its surroundings. Fluctuations of air temperature caused by the hot surface of the analyzer can cause a negative correlation between CO₂

density and the vertical wind speed, resulting in a false sink of CO₂ flux (Burba et al., 2008). The sensor-heating correction (method 4 described in Burba et al., 2008) was applied to all data. Some uncertainties in applying the correction are as follows: (1) the sensor was oriented nearly vertically but not perfectly, whereas the correction method developed by Burba et al. (2008) assumes that the sensor is exactly vertical; (2) we did not measure the temperature of the sensor surface, and it had to be estimated by empirical equations (method 4 in Burba et al. 2008); and (3) the NOAA gas analyzer was used for the measurement in 2007 instead of the LI-7500 gas analyzer, and an appropriate correction for the NOAA gas analyzer is probably different from that for the LI-7500 gas analyzer. Regardless of these uncertainties, we used the same correction as for the LI-7500 to be consistent. The relationship between CO₂ flux with heat correction and CO₂ flux without the heat correction is estimated as follows:

$$F_{cc} \left(\text{g C m}^{-2} \text{ day}^{-1} \right) = 1.03 \times F_{cw} + 0.76 \left(R^2 = 0.99 \right) \quad (1)$$

for the NOAA gas analyzer, and

$$F_{cc} \left(\text{g C m}^{-2} \text{ day}^{-1} \right) = 0.97 \times F_{cw} + 0.89 \left(R^2 = 0.92 \right) \quad (2)$$

for the LI-7500 gas analyzer. F_{cc} is CO₂ flux with heat correction and F_{cw} is CO₂ flux without heat correction. It should be noted that the correction contributed significantly to the mean flux values despite small contributions to the magnitude of the half-hourly flux.

Contamination, especially by sea spray, on the mirror surface of the infrared gas analyzer can potentially cause a false negative correlation between CO₂ density and relative humidity (Prytherch et al., 2010). Prytherch et al. (2010) attributed the high magnitude of the CO₂ flux often observed by the eddy covariance technique over the ocean to this cross sensitivity, and suggested an algorithm to estimate the uncontaminated slope of the CO₂ mixing ratio to humidity. However, our sensors were cleaned at least every 3 days, and the sensitivity of the CO₂ mixing ratio to humidity in our data (~ 0.0025 [mmol_{CO₂}/mol_{air}]/[%_{humid}/100]) was much less than that reported in Prytherch et al. (2010) (~ 0.07 [mmol_{CO₂}/mol_{air}]/[%_{humid}/100]). Else et al. (2011) reported that the application of the cross-sensitivity correction lead to a large scatter in the data. We also encountered the same problem, CO₂ flux with cross-sensitivity correction = $0.63 \times$ CO₂ flux without the correction + 0.80 ($R^2 = 0.15$). Consequently the correction was not applied to our study.

2.2.4 Quality controls

Data quality was assessed using diagnostic values provided by the infrared gas analyzer and the sonic anemometer (9 %: numbers in parentheses indicate the data amount filtered out

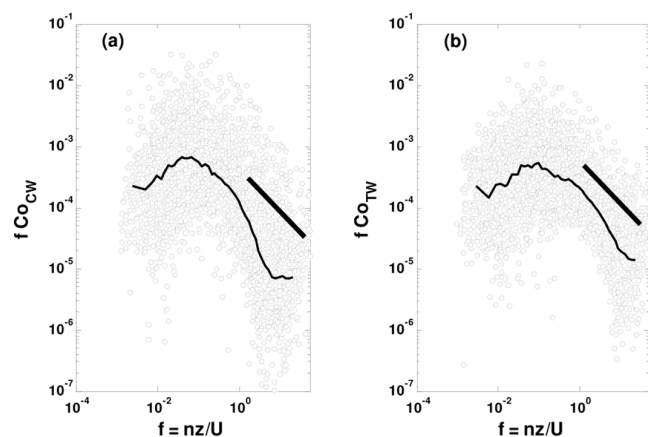


Fig. 2. Normalized cospectra of the vertical wind speed and the CO₂ density, fCo_{Cw} (a) and the vertical wind speed and temperature, fCo_{Tw} (b) for the eddy covariance data obtained at a coastal upwelling site near Bodega Bay, CA. The thin black lines show averages for each frequency and the thick black lines show $-4/3$ at log-log scale.

by each process). After the sonic anemometer data was filtered using the diagnostic value, data during offshore winds, wind directions of $310\text{--}160^\circ$ (where a wind direction of 0° indicates a northerly winds and the degree increases clockwise), were filtered out (39%). The double-differenced time series using the median of absolute deviation about the median was then used to filter out outliers (10%) (Sachs, 1996), with the parameter z in the outlier detector set as 4 (Papale et al., 2006). Finally, apparent outliers (larger than $30\text{ g C m}^{-2}\text{ day}^{-1}$ or lower than $-30\text{ g C m}^{-2}\text{ day}^{-1}$) were also filtered out (1%). After all data filtering processes were complete, 48% of the CO₂ fluxes remained for further analysis.

Cospectra of CO₂ and temperature with the vertical wind speed were evaluated to assess data quality (Fig. 2). Cospectral analysis is generally used to evaluate if any artificial noise resulted in erroneous data and if the sensors reasonably resolved high frequency (e.g., Kondo and Tsukamoto, 2007). When the sensors accurately resolve the high-frequency contributions to the covariance, the logarithmic cospectra of scalar and vertical wind speed follow a $-4/3$ slope against normalized frequency as shown in Fig. 2 (Kaimal et al., 1972). This region of mid- to high-frequency turbulence is known as the inertial subrange, and is predicted by based on the cascade of turbulent energy from relatively large, low-frequency, turbulence into smaller, high-frequency turbulence (Kaimal et al., 1972).

Footprint analysis (Schuepp et al., 1990) performed on the quality-controlled fluxes indicated that 90% of the fluxes originated from within 3 km off the coast. The 30 m of land between the tower base and the ocean accounted for less than 0.01% of the flux footprint, even under conditions with the smallest flux footprint. The water depth

within the footprint area was estimated to be about 20–30 m (Day and Faloon, 2009).

2.3 Environmental data and the Bodega Ocean Observing Node (BOON)

Wind speed and wind direction were measured with the same sonic anemometer used for the eddy covariance measurements. Data sets of air temperature, wind speed, wind direction, photosynthetic photon flux density (PPFD), sea surface temperature (SST), salinity, and chlorophyll density were obtained from the Bodega Ocean Observing Node (BOON, <http://www.bml.ucdavis.edu/>). Air temperature, wind speed, wind direction, and PPFD had been recorded every hour at a meteorological tower located 30 m inland from the intertidal zone ($38^\circ 19' \text{ N}$, $123^\circ 04' \text{ W}$) since 1988, and SST, salinity, and chlorophyll density had been measured on a buoy (BML buoy) located 1.3 km offshore ($38^\circ 18' \text{ N}$, $123^\circ 04' \text{ W}$) from our study site. SST and salinity had been measured since 1988, and chlorophyll data was available only from 2005 to 2008. The $p\text{CO}_2$ was measured every hour by a SAMI- $p\text{CO}_2$ (Sun-Burst Sensors, USA) colorimetric sensor mounted on the buoy from November 2010 to July 2011. The measurement was temporarily halted due to a system malfunction in December 2010 through February 2011. The sensor was calibrated by the factory within the range $150\text{--}700\text{ }\mu\text{atm}$. In addition, the sensor compared well with the $p\text{CO}_2$ system reported in Ikawa and Oechel (2011). All the data used in this study are summarized in Table 1.

2.4 CO₂ flux estimation with $p\text{CO}_2$ and atmospheric CO₂

CO₂ flux (F_c) was calculated from $p\text{CO}_2$ (C_{pw}), SST, salinity, and the atmospheric partial pressure of CO₂ (C_{pa}) with the bulk method for each $p\text{CO}_2$ measurement based on the following equation (e.g., Wanninkhof and McGillis, 1999):

$$F_c = \alpha k [C_{pa} - C_{pw}]. \quad (3)$$

The solubility, α , was computed from SST and salinity based on Weiss (1974); the gas transfer velocity, k , was determined to be the average value calculated following Wanninkhof and McGillis (1999) (hereafter, W&M99), Wanninkhof (1992) (hereafter, W92), Ho et al. (2006) (hereafter, Ho06), Nightingale et al. (2000) (hereafter, N00), and Sweeney et al. (2007) (hereafter, Sw07). The equations for k (m d^{-1}) are as follows:

$$k = 0.0068u^3 \times (Sc/660)^{-0.5}, \quad (4)$$

(W92)

$$k = 0.074u^2 \times (Sc/660)^{-0.5}, \quad (5)$$

(Ho06)

Table 1. Data summary.

Parameter	Date range	Location	Position
Eddy covariance tower			
CO ₂ flux			
Friction velocity	28 May–5 Jun 2007,	Bodega Bay,	38°20' N,
Wind speed	31 Aug–25 Sep 2008	CA	123°04' W
Wind direction			
BML meteorological tower			
Air temperature			
Wind speed	1988–2011	Bodega Bay,	38°19' N,
Wind direction		CA	123°04' W
PPFD			
BML buoy			
Sea surface temperature			
Salinity	1988–2011	Near Bodega	38°18' N,
Chlorophyll density	2007–2008	Bay, CA	123°04' W
pCO ₂	Nov 2010–Jul 2011		
NDBC 40613 buoy			
Wind speed			
Wind direction		Near Bodega	38°14' N,
AWV (calculated from	2007–2011	Bay, CA	123°18' W
WS and WD)			
Sea surface temperature			
Aircraft CO ₂ measurement			
Atmospheric CO ₂	Sep 2003–Jan 2012	Near Trinidad	41°05', 124°17' W
		Head, CA	(~ 4 km in altitude)

$$k = 0.061u^2 \times (Sc/660)^{-0.5}, \quad (6)$$

(N00)

$$k = [0.053u^2 + 0.024u] \times (Sc/660)^{-0.5}, \quad (7)$$

(Sw07)

$$k = 0.065u^2 \times (Sc/660)^{-0.5}, \quad (8)$$

where, u is wind speed and Sc is the Schmidt number (Wanninkhof, 1992).

Data collected monthly by the NOAA/ESRL Carbon Cycle Greenhouse Gases (CCGG) group's aircraft program were used to estimate the atmospheric partial pressure of CO₂. The nearest routine sampling location is offshore near Trinidad Head, CA, which is located about 300 km north of Bodega Bay (~ 41°10' N, 124°20' W). The lowest altitude data (near 300 m a.s.l.) from each month since September, 2003 were used to estimate the average monthly atmospheric CO₂ concentration in the marine boundary layer throughout the region. The CO₂ concentration was then converted to units of pressure based on the standard atmosphere.

2.5 Effective upwelling and National Data Buoy Center 46013 data

The National Data Buoy Center (NDBC) 46013 buoy is located off of Bodega Bay, California (38°14' N, 123°18' W). The Effective Upwelling Index (EUI) was introduced by Garcia-Reyes (2011) as a proxy for the cumulative NO₃. It is estimated using the sea surface temperature measured at the NDBC 46013 buoy (SST_{N13}) from the National Data Buoy Center (<http://www.ndbc.noaa.gov>). To identify upwelling periods, NO₃ concentrations were estimated based on the NO₃–SST_{N13} relation (Garcia-Reyes, 2011). EUI was then calculated as a summation of a temporal differential of NO₃ estimated while the daily averaged alongshore wind velocity was greater than 5 m s⁻¹. EUI was set back to zero when the daily alongshore wind velocity was less than 5 m s⁻¹ for over 3 days. Alongshore wind velocity was calculated by multiplying cos (wind direction – the angle of the coast) to wind speed. The angle of the coast was 315°.

2.6 Statistic analysis

2.6.1 For the eddy covariance data set

A *t* test was used to test the significance of differences between the 2007 and 2008 CO₂ fluxes and environmental parameters (i.e., SST, salinity, PPF, wind speed, alongshore wind velocity, friction velocity, chlorophyll density).

2.6.2 For the pCO₂ data set

Linear correlation analysis was used to investigate relationships between environmental parameters (i.e., SST, salinity, PPF, wind speed and alongshore wind velocity) and pCO₂ and CO₂ fluxes calculated from pCO₂. Since diurnal variations in pCO₂ were minimal (less than 10% of the total variations), these data were averaged for 24 h periods.

2.7 Estimates of dissolved inorganic carbon (DIC) and cumulative monthly CO₂ flux and net primary production (NPP)

To evaluate the monthly net CO₂ exchange between the air–water interface and the monthly net primary production (NPP) and to compare them with the dissolved inorganic carbon (DIC) pool, monthly CO₂ fluxes and NPP were roughly estimated and compared with estimated DIC per unit area within the surface mixed layer for the years from 1988 to 2011. CO₂ fluxes were estimated with the bulk method explained above. pCO₂ during this period was estimated with a multiple linear regression with environmental parameters with good correlation.

$$C_{pw} = \beta_0 + \beta_1 P_1 + \beta_2 P_2 + \beta_3 P_3 + \dots + \beta_n P_n, \quad (9)$$

where, $\beta_0 - \beta_n$ and $P_1 - P_n$ are environmental parameters, n is the number of parameters that were significantly correlated to pCO₂ at ($p < 0.001$). DIC (C_{dic}) was computed based on the estimated pCO₂, SST, salinity and pH (324–325 in Sarmiento and Gruber, 2006):

$$C_{dic} = C_{pw} K_0 \left[1 + K_1 [H^+]^{-1} + K_1 K_2 [H^+]^{-2} \right], \quad (10)$$

where, K_0 is the solubility of CO₂ (mol kg⁻¹ atm⁻¹), K_1 and K_2 are dissociation constants of inorganic carbon species (mol kg⁻¹) determined from temperature and salinity, and $[H^+]$ is hydrogen ion concentration (mol kg⁻¹) and equal to 10^{-pH}. Hauri et al. (2012) reported seasonal cycles of pH off the central California coast, and based on their results we approximated the pH seasonal cycle with a sine curve. The influence of the seasonal variation of pH on the DIC calculation was minimal (less than 3%). Similarly, the NPP off central California reported in Kahru and Mitchell (2002) was approximated by a sine curve. The surface mixed layer depth was approximated by wind stress estimated from wind speed (Lentz, 1992).

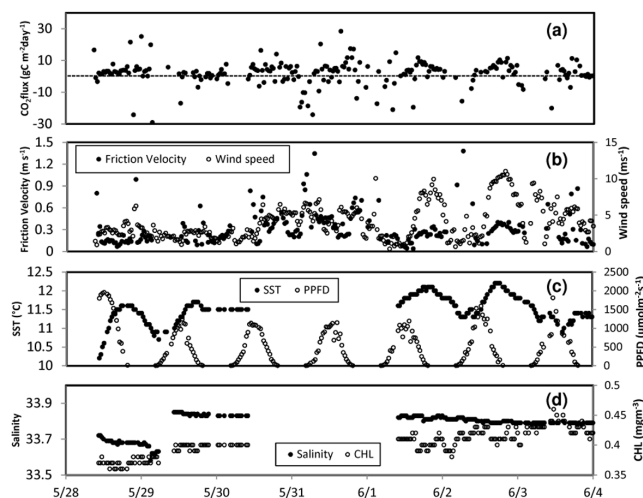


Fig. 3. CO₂ flux (a), friction velocity and wind speed (b), sea surface temperature (SST) and photosynthetic photon flux density (PPFD) (c), and salinity and chlorophyll density (CHL) (d) measured at a coastal upwelling site off of Bodega Bay, CA from 28 May to 4 June 2007. All data were plotted every 30 min.

To quantify the variability in the estimated CO₂ flux and DIC due to different regression fittings in Eq. (9) owing to different data sampling, the data set of pCO₂ and environmental parameters was reconstructed 100 times by bootstrapping and regression coefficients were determined each time. Then, the maximum and minimum values of the estimated CO₂ flux and DIC out of the 100 estimates were considered as the 99% upper and lower confidence intervals, respectively.

3 Results and discussions

High CO₂ efflux to the atmosphere was observed during the measurement period in 2007. The average CO₂ flux during this period was 1.5 (±7 SD) gC m⁻² day⁻¹ with high variability (Fig. 3a, Table 2). Although a relatively strong sink of CO₂ was observed with high wind speeds on 7–12 September 2008, the overall CO₂ flux measured in 2008 was a slight source of CO₂, with a magnitude of 0.2 (±3 SD) gC m⁻² day⁻¹ (Fig. 4a, Table 2), and the average CO₂ flux during the 2008 measurement season was not significantly different from zero (Table 2).

Contrasting differences were found in SST, salinity, and chlorophyll density between the 2007 and 2008 measurement seasons (Table 2). No difference in alongshore wind velocity between the 2007 and 2008 measurement periods was apparent. However, alongshore wind velocity on longer time scales strengthened in late spring to early summer corresponding with a drop in sea surface temperatures (Fig. 5a, b). The alongshore wind velocity typically weakens in the fall leading to an increase in sea surface temperature (Garcia-Reyes, 2011). A high EUI (~20 μM) was still observed during fall

Table 2. Mean, standard deviation, maximum, and minimum of CO₂ flux (F_c) in g C m⁻² day⁻¹, wind speed (U) in m s⁻¹, friction velocity (U^*) in m s⁻¹, air temperature (T_a) in °C, PPF_D in μmol m⁻² s⁻¹, chlorophyll density (CHL) in mg m⁻³, salinity (SS) in unitless, sea surface temperature (SST) in °C, sea surface temperature measured at the NDBC 46013 buoy (SST_{N13}) in °C and alongshore wind velocity (AWV) in m s⁻¹ from (A) 28 May–4 June 2007 and (B) 30 August–24 September 2008. ^a Statistically significant difference between the periods (A) and (B) in each parameter ($p < 0.01$). ^b not statistically different from zero at $p = 0.01$.

(A) 28 May–4 June 2007										
	F_c	U	U^*	T_a	PPFD	CHL	SS	SST	SST _{N13}	AWV
Mean	1.5	4.5	0.33	13.6	609	0.4	34	11.5	10.3	2.6
Standard deviation	7.4	2.7	0.3	3.2	522	0.0	0.5	0.4	0.6	2.0
Maximum	28.3	11.7	2.52	21.9	2011	0.5	34	12.2	12.4	9.3
Minimum	-29.1	0.6	0.04	8.3	0	0.0	28	9.6	9.1	0.1
(B) 30 August–24 September 2008										
	F_c	U	U^*	T_a	PPFD	CHL	SS	SST	SST _{N13}	AWV
Mean	0.2 ^b	2.8	0.19	12.5	523	1.8	32	16.8	14.0	3.9
Standard deviation	2.5	1.4	0.1	1.2	484	0.7	0.2	0.3	1.0	4.7
Maximum	16.5	8.1	1.82	16.4	1645	3.5	33	17.7	17.5	17.0
Minimum	-21.0	0.2	0.02	10.7	0	0.7	32	15.9	11.7	-5.8
	a	a	a	a		a	a	a	a	

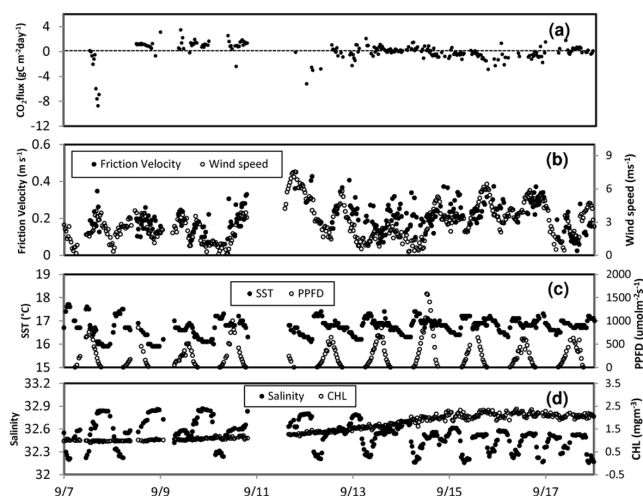


Fig. 4. CO₂ flux (a), friction velocity and wind speed (b), sea surface temperature (SST) and photosynthetic photon flux density (PPFD) (c), and salinity and chlorophyll density (CHL) (d) measured at a coastal upwelling site off of Bodega Bay, CA from 30 August to 24 September 2008. All data were plotted every 30 min.

2008, but a negative alongshore wind velocity (~ -5 m s⁻¹) was frequently observed, creating conditions favorable to relaxation (Fig. 5a, c). The relatively lower SSTs ranging from 10 to 12 °C in May–June 2007 and higher SSTs ranging from 15 to 18 °C in August–September 2008 shown in Fig. 5b are compatible with the typical seasonal variations in SST, where upwelling intensifies in early summer and relaxes in fall (Garcia-Reyes, 2011). The upwelling season is

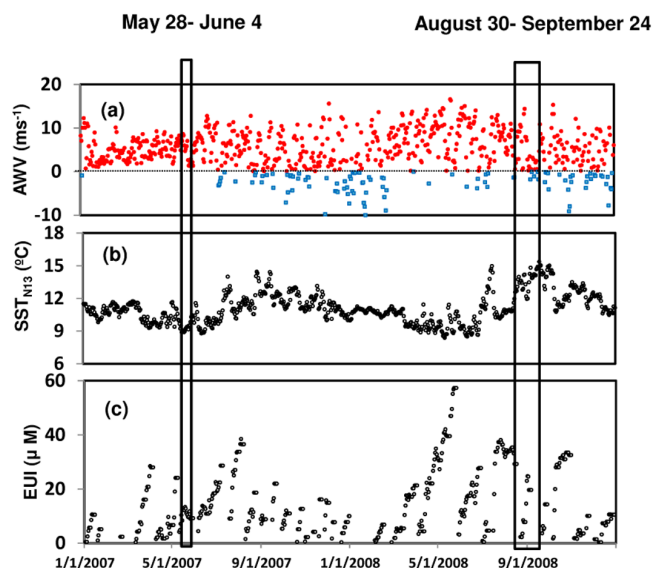


Fig. 5. Alongshore wind velocity (AWV) calculated from wind speed and directions at the NDBC 46013 buoy, with positive AWV (red dots) and negative AWV (blue dots) differentiated by color (a), sea surface temperature at the NDBC 46013 buoy (SST_{N13}) (b), and effective upwelling index (EUI) (c). All data were averaged daily and plotted. The two boxes indicate the periods when eddy covariance measurements were available.

also characterized by high temporal variations in CO₂ flux, which was also observed in the 2007 measurements, due to the highly dynamic shifts of water chemistry caused by upwelled water with high CO₂ and subsequent CO₂ uptake by

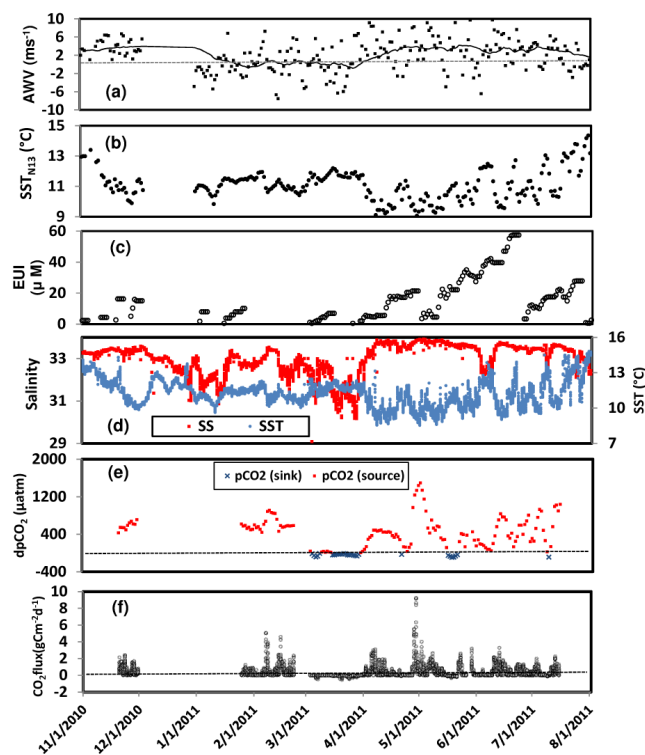


Fig. 6. Hourly alongshore wind velocity (AWV) calculated from wind speed and direction at the NDBC 46013 buoy (black squares), with the 30 point running average (black line) also shown (a), sea surface temperature at the NDBC 46013 buoy (SST_{N13}) (b), and effective upwelling index (EUI) (c), salinity and sea surface temperature (SST) (d), ΔpCO_2 (pCO_2 – atmospheric CO_2) (e) and CO_2 flux estimated by the bulk method for a coastal upwelling site near Bodega Bay (f) from November 2010 to July 2011. (a–c) were plotted daily and (d–f) were plotted hourly.

primary production (Dugdale et al., 2006; Evans et al., 2011; Gago et al., 2003).

Relaxation periods are favorable to stratification of the upper water column, which was reflected in lower salinity (~ 32) and higher SST ($\sim 17^\circ C$) during the 2008 measurement period. Stratification further enhances nutrient depletion on the surface and increases primary production, resulting in higher chlorophyll density. Interestingly, an increasing trend of chlorophyll density was observed during the 2008 measurement period (Fig. 4d). A sink of CO_2 , $\sim 2 g C m^{-2} day^{-1}$ was consistently observed on 15 September 2008, when chlorophyll density approached the maximum of $2.3 mg m^{-3}$. The measurement period in 2008 fell directly between high upwelling events with the peaks of EUI in mid-July and October 2008 (Fig. 5c). Therefore, high nutrient levels were brought to the surface by the preceding upwelling event, increasing the chlorophyll density until the nutrients were depleted. Kahru and Mitchell (2002) reported high NPP of $2.4 g C m^{-2} day^{-1}$ (ca. $5 \times 10^{12} g C month^{-1}$ for the area of $6.2 \times 10^4 km^2$) in summer when nutrient availability was

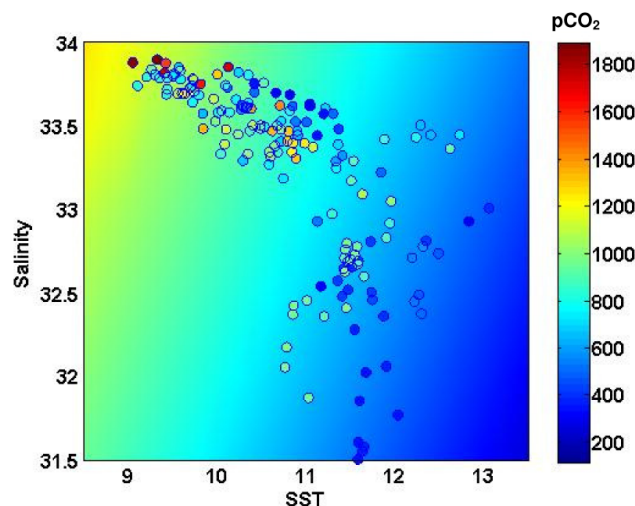


Fig. 7. Distribution of daily averaged pCO_2 (μatm) in relation to salinity and sea surface temperature (SST) ($^\circ C$) measured at a coastal upwelling site near Bodega Bay from November 2010 to July 2011. A multiple linear regression was applied for pCO_2 against both salinity and SST ($R = 0.57$, $p < 0.001$). The background color shows pCO_2 estimated from the multiple linear regressions at given salinity and SST.

high near our study site. However, the overall CO_2 flux was near zero or a slight source during the 2008 measurement period despite the favorable conditions for biological CO_2 uptake. This was because the period preceded another high upwelling period that stimulated higher chlorophyll density and probable relaxation conditions, as inferred from the negative alongshore wind velocity.

The overall CO_2 flux estimated from ΔpCO_2 was also a source of $0.4 (\pm 0.6 SD) g C m^{-2} day^{-1}$ from November 2010 to July 2011 (Fig. 6f). The pCO_2 data were often out of the calibration range (150–700 μatm), and therefore the data may not have been accurate at higher pCO_2 values (Fig. 6e). However, pCO_2 higher than 1000 μatm is likely in our study area (personal communication with Dr. John Largier of University of California, Davis, 2007). Correlation analysis showed that pCO_2 was most correlated with SST ($R = -0.54$, $p < 0.001$) followed by salinity ($R = 0.50$, $p < 0.001$), and CO_2 flux was strongly correlated to wind speed ($R = 0.58$, $p < 0.001$) and alongshore wind velocity ($R = 0.51$, $p < 0.001$) followed by SST ($R = -0.40$, $p < 0.001$) and salinity ($R = 0.34$, $p < 0.001$). Similar to the flux data obtained by the eddy covariance technique, higher salinity and lower SST corresponded with higher pCO_2 and a source of CO_2 (Fig. 7). Equation (9) is rewritten as

$$C_{pw} = -1473 - 142S_T + 115S_s, \quad (11)$$

where S_T is SST and S_s is salinity. The correlation between SST and salinity decreased at lower salinity (below 33) and higher temperature (above $12^\circ C$). The low salinity below 33 was almost exclusively observed between December 2010

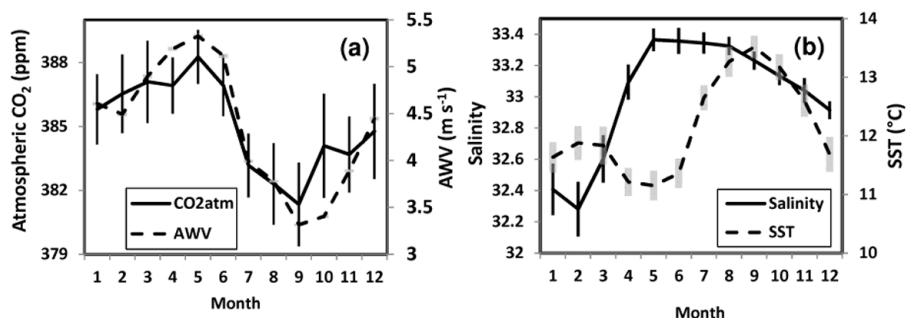


Fig. 8. Average seasonal variations of atmospheric CO₂ concentration between September 2003 to August 2012 obtained near Trinidad Head, CA and alongshore wind velocity (AWV) between 1988 to 2011 (a) and average seasonal variations of salinity and sea surface temperature (SST) from 1988 to 2011 obtained from the BML buoy (b). Vertical bars show standard errors (SE). The average and SE for each month were calculated from the monthly averages available for all years.

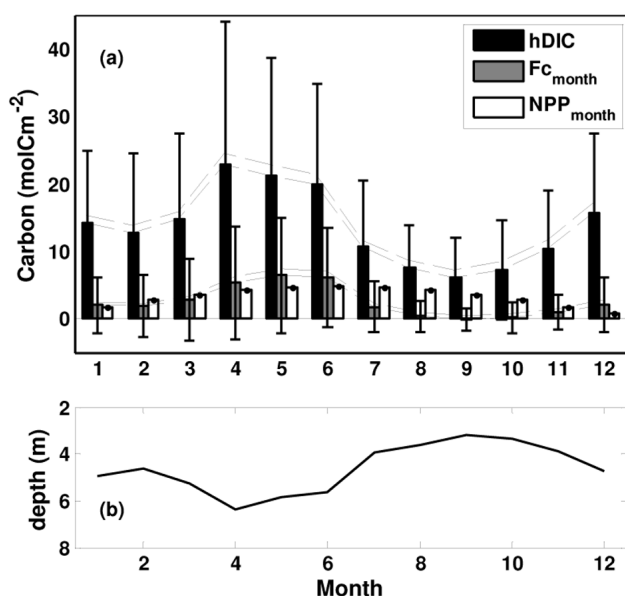


Fig. 9. Monthly averaged seasonal variations of DIC per unit area within the surface mixed layer (hDIC), monthly CO₂ flux ($F_{c,month}$), and monthly NPP (NPP_{month}) (a) and the depth of the surface-mixed layer depth (b) estimated from 1988 to 2011 data for a coastal upwelling zone near Bodega Bay. The vertical lines indicate standard deviations. Dashed lines indicate 99 % confidence intervals of the estimated hDIC and $F_{c,month}$ due to the variability in the regression coefficients in Eq. (9) determined from different data sampling.

and March 2011 (Fig. 6). Alongshore wind velocity tended to be negative during this period. This period with southerly wind (“reversal winds” Garcia-Reyes (2011) led to weak upwelling, associated with low salinity at the surface caused by decreased vertical mixing.

Salinity and SST buoy data from 1988 to 2011 showed that the annual variation of salinity reached its maximum level and SST reached its minimum level concurrently, as

the alongshore wind velocity peaked during the upwelling season in late spring and early summer (Fig. 8). Therefore, although alongshore wind velocity did not reflect CO₂ flux on short time scales (~ 1 h), it likely reflected CO₂ flux on a seasonal scale. Interestingly, the seasonal change of the atmospheric CO₂ showed a very similar pattern to alongshore wind velocity (Fig. 8a) with a higher peak during a high upwelling season in late spring to early summer; however, because the atmospheric changes in CO₂ concentration were so much smaller than those induced in the ocean surface, this periodicity did not influence the overall flux significantly.

The CO₂ flux estimated from the eddy covariance technique and from the bulk method both showed that positive CO₂ fluxes were larger than negative fluxes, and that this balance was tightly reflected in salinity and SST. The fact that 99 % of the historical salinity and SST data fell within the range of our observations indicates that the observations were representative of the region in general. Our data indicate that the overall exchange of CO₂ in this area is likely a net source of CO₂ to the atmosphere. Table 3 lists our CO₂ flux data together with the CO₂ flux in upwelling zones reported in past studies. Although the annual net CO₂ flux in some upwelling zones (e.g., the North Pacific and Galician coast) show a sink of CO₂ and high primary production, other studies conducted in north-central California (Feely et al., 2008; Friederich et al., 2002; Wilkerson et al., 2006) further support our conclusion that the upwelling zone off of Bodega Bay is an overall source of CO₂ to the atmosphere. Despite the high chlorophyll density of 11 mg m⁻³ observed in the early summer of 2000 by Wilkerson et al. (2006), their pCO_2 measurements still indicated that the area was a source of CO₂ to the atmosphere (Table 3).

The estimate of CO₂ flux and DIC based on the relationship of pCO_2 with SST and salinity revealed that the monthly CO₂ flux reached its maximum in May (~ 7 mol C m⁻² month⁻¹), which is equal to about 30 % of DIC within the surface mixed layer (Fig. 9). The annual CO₂ flux was estimated to be about 35 mol C m⁻² yr⁻¹. The variations in

Table 3. CO₂ flux, *p*CO₂, wind speed, sea surface temperature (SST), salinity (SS) and chlorophyll density (CHL) observed in coastal upwelling zones.

Location	Time	CO ₂ flux mol C m ⁻² yr ⁻¹	<i>p</i> CO ₂ µatm	Wind Speed m s ⁻¹	SST °C	SS psu	CHL mg m ⁻³	Technique	Study
Peruvian and Chilean coast									
Cabo Nazca, Peru	Spring 76	7 ^a	120–980	–	19–23	–	2–31	Bulk	Simpson and Zirino (1980)
Peruvian coast	Aug 86	20 ^a	400–1000	–	15–17	35	2	Bulk	Copin-Montegut and Raimbault (1994)
Chilean coast	Jan 96	20 ^a	300–900	–	13–19	34–35	–	Bulk	Torres et al. (1999)
Arabian coast									
Arabian Sea	95	0.3	+10–+50 ^b	–	20–30	–	–	Bulk	Goyet et al. (1995)
Oman coast	Jul 97	14	+260 ^b	0–18	22–31	36	0–2	Bulk	Lendt et al. (2003)
North Pacific									
St. Lawrence Island	Summer 68	10 ^a	+110 ^b	–	5	–	–	Bulk	Kelley and Hood (1971)
Oregon coastal ocean	May–Aug 01	–7	180–600	0–15	8–11	32–33	–	Bulk	Hales et al. (2005)
Oregon coastal ocean	07–10	–0.3	100–1100	–15–15 ^c	8–16	26–34	0–5	Bulk	Evans et al. (2011)
Vancouver Island, Canada	typical year	–0.5	–	–	–	–	–	BM	Ianson and Allen (2002)
North Pacific	typical year	–2	–	–	–	–	–	BM	Ianson et al. (2009)
Galician coast									
Galician coast, Spain	97–99	–2	270–420	–	15–20	35	–	Bulk	Borges and Frankignoulle (2002)
NW Spain	Apr–Dec 97	–0.1	300–370	–	12–18	33–35	–	Bulk	Gago et al. (2003)
N-C California coast									
Central California coast	98–00	2	–200–+300 ^b	–	9–17	–	–	Bulk	Friederich et al. (2002)
Pt. St George, CA	Summer 07	40 ^a	800–1100	–	–	–	–	Bulk	Feely et al. (2008)
Bodega Bay, CA	1–3 Jun 00	9 ^a	450–550	3–10 ^c	9–10	34	10–12	Bulk	Wilkerson et al. (2003)
Bodega Bay, CA	19–20 May 01	20 ^a	600–650	1–11 ^c	10–11	34	3–4	Bulk	Wilkerson et al. (2003)
Bodega Bay, CA	15–17 Jun 02	40 ^a	750–850	9–10 ^c	9–10	34	1.5	Bulk	Wilkerson et al. (2003)
Bodega Bay, CA	May–Jun 07	46	–	4.5	12	34	0.4	EC	This study
Bodega Bay, CA	Sep 08	6	–	2.8	17	32	1.8	EC	This study
Bodega Bay, CA	10–Jul Nov 11	12	+400 ^b	5.0	11	33	–	Bulk	This study

^a CO₂ flux estimated by reported *p*CO₂ with the bulk method (average of Nightingale et al., 2000 and Wanninkhof, 1992); ^b *d**p*CO₂ (atmospheric CO₂–*p*CO₂); ^c Alongshore wind velocity.

the estimated monthly CO₂ flux and DIC within the surface mixed layer due to the variations in the regression fittings were small (less than 10 %) and much less than the year-to-year variations. The fraction of monthly NPP to DIC within the surface mixed layer became highest (~ 50 %) in late summer, and the annual NPP was estimated to be about 40 mol C m⁻² yr⁻¹. This simple estimate suggests that CO₂ flux and NPP were about the same magnitude and together accounted for significant flux compared to the stock of DIC.

A challenge remains in the evaluation of the extent to which our study area is spatially representative. Wilkerson et al. (2006) shows that the magnitude of high *p*CO₂ near our study site was similar at least along the cross-shelf distance of 50 km offshore (Figs. 3, 8, and 13 in Wilkerson et al., 2006). Their data also show that the spatial distribution of relatively higher *p*CO₂ was associated with higher salinity and lower temperature, and vice versa (Wilkerson et al., 2006). However, the representativeness of the alongshore distance still remains in question. Despite a strong upwelling zone relatively close to our study site, the North Pacific is estimated to be a sink of CO₂ (Evans et al., 2011; Hales et

al., 2005), and the coastal sea off western North America is roughly estimated to be a sink of CO₂ overall (Ikawa, 2013). Borges (2011) suggests that the extent to which a coastal upwelling zone releases CO₂ depends on whether the upwelled water originates from an oxygen minimum zone where dissolved oxygen concentration is below 0.5 mg O₂ L⁻¹. Understanding the trajectory of upwelling current may help further understand alongshore variations of CO₂ flux within and near-coastal upwelling zones.

4 Summary

The CO₂ flux from the coastal waters of Bodega Bay was measured during a typical upwelling season in 2007 and during a relaxation season in 2008. CO₂ flux was also estimated from *p*CO₂ measured from November 2010 to July 2011. Contrasting patterns in CO₂ flux and environmental parameters were observed between the two measurement periods in 2007 and 2008. Measurements in 2007 were during a typical upwelling period, as indicated by the seasonal variations

of alongshore wind velocity and EUI in early summer, and a source of CO₂ to the atmosphere was observed concurrently with low SST, high salinity, and low chlorophyll density. The measurements in 2008 were, on the contrary, made during a relaxation period with high SST and low salinity that likely led to water stratification and high chlorophyll density. A strong upwelling event preceding the measurements in 2008 likely created favourable conditions for CO₂ uptake. However, the average CO₂ flux over the 2008 measurements was a small source of CO₂ overall. The *p*CO₂ measurements also indicated that the coastal waters were a net source of CO₂ to the atmosphere. Similar to the fluxes observed by the eddy covariance technique, those estimated by the *p*CO₂ measurements were closely related to salinity and SST. The historical salinity and SST data set (1988–2011) indicated that 99% of the data fell within the range of our observations. Therefore, the area was likely a source of CO₂ to the atmosphere annually. Past studies further support the assertion that the prevailing conditions in the coastal upwelling area off of Bodega Bay are favourable to producing a source of CO₂. This is true to in the region at least within 50 km off the coast. Although alongshore wind velocity did not reflect *p*CO₂ or CO₂ flux on shorter time scales, high alongshore wind velocity together with low SST and high salinity suggests that alongshore wind velocity likely drives the seasonal cycle of CO₂ flux. Based on the *p*CO₂ to SST and salinity relationship, the average annual CO₂ flux between 1988 and 2011 was estimated to be 35 mol C m⁻² yr⁻¹, and the amount of CO₂ emitted to the atmosphere and consumed due to NPP accounted for a significant fraction of the carbon in the DIC pool within the surface mixed layer.

Acknowledgements. We thank Jackie Sones, Deedee Shideler and logistic supports by Bodega Bay Marine Laboratory, Tessa Hill for *p*CO₂ data retrieval, Joseph Verfaillie for valuable suggestions on data processing and interpretation, and four anonymous referees whose comments largely improved our manuscript. Sea surface temperature, wind speed and wind direction for calculating EUI was provided by the National Data Buoy Center. SAMI-*p*CO₂ data were provided by the Bodega Ocean Acidification Research group (NSF OCE No. 0927255 to B. Gaylord), and Bodega Ocean Observing Network (BOON) data were provided by John Largier. Atmospheric CO₂ data from the NOAA/ESRL Carbon Cycle Greenhouse Gases group were provided by Colm Sweeney. Partial support for KTPU was from NSF/MIT sub-award 5710003122.

Edited by: M. Dai

References

- Auble, D. L. and Meyers, T. P.: An open path, fast response infrared absorption gas analyzer for H₂O and CO₂, *Bound.-Lay. Meteorol.*, 59, 243–256, doi:10.1007/BF00119815, 1992.
- Bakun, A.: Global Climate Change and Intensification of Coastal Ocean Upwelling, *Science*, 247, 198–201, doi:10.1126/science.247.4939.198, 1990.
- Borges, A. V.: Present Day Carbon Dioxide Fluxes in the Coastal Ocean and Possible Feedbacks Under Global Change, in: *Oceans and the Atmospheric Carbon Content*, edited by: Duarte, P. and Santana-Casiano, J. M., 47–77, Springer, the Netherlands, 2011.
- Borges, A. V. and Frankignoulle, M.: Distribution of surface carbon dioxide and air-sea exchange in the upwelling system off the Galician coast, *Global Biogeochem. Cy.*, 16, 1020, doi:10.1029/2000GB001385, 2002.
- Burba, G. G. and Anderson, D. J.: *A brief Practical Guide to Eddy Covariance Flux Measurements: Principles and Workflow Examples for Scientific and Industrial Applications*, Li-COR Biosciences, Lincoln, USA, 2010.
- Burba, G. G., McDermitt, D. K., Grelle, A., Anderson, D. J., and Xu, L.: Addressing the influence of instrument surface heat exchange on the measurements of CO₂ flux from open-path gas analyzers, *Glob. Change Biol.*, 14, 1854–1876, doi:10.1111/j.1365-2486.2008.01606.x, 2008.
- Chen, C.-T. A. and Borges, A. V.: Reconciling opposing views on carbon cycling in the coastal ocean: Continental shelves as sinks and near-shore ecosystems as sources of atmospheric CO₂, *Deep-Sea Res. Pt. II*, 56, 578–590, doi:10.1016/j.dsr2.2009.01.001, 2009.
- Copin-Montegut, C. and Raimbault, P.: The Peruvian upwelling near 15° S in August 1986. Results of continuous measurements of physical and chemical properties between 0 and 200 m depth, *Deep-Sea Res. Pt. I*, 41, 439–467, 1994.
- Day, D. A. and Faloona, I.: Carbon monoxide and chromophoric dissolved organic matter cycles in the shelf waters of the northern California upwelling system, *J. Geophys. Res.*, 114, C01006, doi:10.1029/2007JC004590, 2009.
- Diffenbaugh, N. S., Snyder, M. A., and Sloan, L. C.: Could CO₂-Induced Land-Cover Feedbacks Alter Near-Shore Upwelling Regimes?, *PNAS*, 101, 27–32, doi:10.1073/pnas.0305746101, 2004.
- Doney, S. C., Tilbrook, B., Roy, S., Metzl, N., Le Quééré, C., Hood, M., Feely, R. A., and Bakker, D.: Surface-ocean CO₂ variability and vulnerability, *Deep-Sea Res. Pt. II*, 56, 504–511, doi:10.1016/j.dsr2.2008.12.016, 2009.
- Dorman, C. E., Holt, T., Rogers, D. P., and Edwards, K.: Large-Scale Structure of the June–July 1996 Marine Boundary Layer along California and Oregon, *Month. Weather Rev.*, 128, 1632–1652, doi:10.1175/1520-0493(2000)128<1632:LSSOTJ>2.0.CO;2, 2000.
- Dugdale, R. C., Wilkerson, F. P., Hogue, V. E., and Marchi, A.: Nutrient controls on new production in the Bodega Bay, California, coastal upwelling plume, *Deep-Sea Res. Pt. II*, 53, 3049–3062, doi:10.1016/j.dsr2.2006.07.009, 2006.
- Else, B. G. T., Papakyriakou, T. N., Galley, R. J., Drennan, W. M., Miller, L. A., and Thomas, H.: Wintertime CO₂ fluxes in an Arctic polynya using eddy covariance: Evidence for enhanced air-sea gas transfer during ice formation, *J. Geophys. Res.*, 116, C00G03, doi:10.1029/2010JC006760, 2011.

- Evans, W., Hales, B., and Strutton, P. G.: Seasonal cycle of surface ocean $p\text{CO}_2$ on the Oregon shelf, *J. Geophys. Res.*, 116, C05012, doi:10.1029/2010JC006625, 2011.
- Feely, R. A., Sabine, C. L., Hernandez-Ayon, J. M., Ianson, D., and Hales, B.: Evidence for Upwelling of Corrosive “Acidified” Water onto the Continental Shelf, *Science*, 320, 1490–1492, doi:10.1126/science.1155676, 2008.
- Foken, T. and Wichura, B.: Tools for quality assessment of surface-based flux measurements, *Agric. Forest Meteorol.*, 78, 83–105, 1996.
- Frew, N. M., Bock, E. J., Schimpf, U., Hara, T., Haußecker, H., Edson, J. B., McGillis, W. R., Nelson, R. K., McKenna, S. P., Uz, B. M., and Jähne, B.: Air-sea gas transfer: Its dependence on wind stress, small-scale roughness, and surface films, *J. Geophys. Res.*, 109, C08S17, doi:10.1029/2003JC002131, 2004.
- Friederich, G. E., Walz, P. M., Burczynski, M. G., and Chavez, F. P.: Inorganic carbon in the central California upwelling system during the 1997–1999 El Niño-La Niña event, *Prog. Oceanogr.*, 54, 185–203, 2002.
- Gago, J., Gilcoto, M., Pérez, F., and Ríos, A.: Short-term variability of $f\text{CO}_2$ in seawater and air–sea CO₂ fluxes in a coastal upwelling system (Ría de Vigo, NW Spain), *Mar. Chem.*, 80, 247–264, doi:10.1016/S0304-4203(02)00117-2, 2003.
- García-Reyes, M.: Variability in Coastal Upwelling off Central and Northern California, Doctoral dissertation of the University of California, Davis, 2011.
- García-Reyes, M. and Largier, J.: Observations of increased wind-driven coastal upwelling off central California, *J. Geophys. Res.*, 115, C04011, doi:10.1029/2009JC005576, 2010.
- Gattuso, J. P., Frankignoulle, M., and Wollast, R.: Carbon and carbonate metabolism in coastal aquatic ecosystems, *Annu. Rev. Ecol. Syst.*, 29, 405–434, 1998.
- Goyet, C., Millero, F. J., O’Sullivan, D. W., Eiseheid, G., McCue, S. J., and Bellerby, R. G. J.: Temporal variations of $p\text{CO}_2$ in surface seawater of the Arabian Sea in 1995, *Deep-Sea Res. Pt. I*, 45, 609–623, 1998.
- Gruber, N., Gloor, M., Fletcher, S. E. M., Doney, S. C., Dutkiewicz, S., Follows, M. J., Gerber, M., Jacobson, A. R., Joos, F., Lindsay, K., Menemenlis, D., Mouchet, A., Müller, S. A., Sarmiento, J. L., and Takahashi, T.: Oceanic sources, sinks, and transport of atmospheric CO₂, *Global Biogeochem. Cycles*, 23, GB1005, doi:10.1029/2008GB003349, 2009.
- Hales, B., Takahashi, T., and Bandstra, L.: Atmospheric CO₂ uptake by a coastal upwelling system, *Global Biogeochem. Cy.*, 19, GB1009, doi:10.1029/2004GB002295, 2005.
- Hauri, C., Gruber, N., Vogt, M., Doney, S. C., Feely, R. A., Lachkar, Z., Leinweber, A., McDonnell, A. M. P., Munnich, M., and Plattner, G.-K.: Spatiotemporal variability and long-term trends of ocean acidification in the California Current System, *Biogeosciences Discussions*, 9, 10371–10428, doi:10.5194/bgd-9-10371-2012, 2012.
- Ho, D. T., Law, C. S., Smith, M. J., Schlosser, P., Harvey, M., and Hill, P.: Measurements of air-sea gas exchange at high wind speeds in the Southern Ocean: Implications for global parameterizations, *Geophys. Res. Lett.*, 33, 16611, doi:10.1029/2006GL026817, 2006.
- Ianson, D. and Allen, S. E.: A two-dimensional nitrogen and carbon flux model in a coastal upwelling region, *Global Biogeochem. Cy.*, 16, p. 1011, 2002.
- Ianson, D., Feely, R. A., Sabine, C. L., and Juranek, L. W.: Features of coastal upwelling regions that determine net air-sea CO₂ flux, *J. Oceanogr.*, 65, 677–687, 2009.
- Ikawa, H.: Air-sea CO₂ exchange of the coastal marine zone. Doctoral dissertation of the Joint Doctoral Program in Ecology of University of California, Davis and San Diego State University, University of California, Davis and San Diego State University, March, 2013.
- Ikawa, H. and Oechel, W. C.: Air–sea CO₂ exchange of beach and near-coastal waters of the Chukchi Sea near Barrow, Alaska, *Cont. Shelf Res.*, 31., 1357–1364, doi:10.1016/j.csr.2011.05.012, 2011.
- Iwata, T., Yoshikawa, K., Higuchi, Y., Yamashita, T., Kato, S., and Ohtaki, E.: The Spectral Density Technique for the Determination of CO₂ Flux Over the Ocean, Bound-Lay. Meteorol., 117, 511–523, doi:10.1007/s10546-005-2773-4, 2005.
- Jähne, B., Münnich, K. O., Dutzi, R. B. A., Huber, W., and Libner, P.: On the Parameters Influencing Air-Water Gas Exchange, *J. Geophys. Res.*, 92, 1937–1949, doi:10.1029/JC092iC02p01937, 1987.
- Kahru, M. and Mitchell, B. G.: Influence of the El Niño-La Niña cycle on satellite-derived primary production in the California Current, *Geophys. Res. Lett.*, 29, 1846, doi:10.1029/2002GL014963, 2002.
- Kaimal, J. C., Wyngaard, J. C., Izumi, Y., and Cote, O. R.: Spectral characteristics of surface-layer turbulence, *Quart. J. Roy. Meteorol. Soc.*, 98, 563–589, 1972.
- Keeling, R. F.: On the role of large bubbles in air-sea gas exchange and supersaturation in the ocean, *J. Mar. Res.*, 51, 237–271, doi:10.1357/0022240933223800, 1993.
- Kelley, J. J. and Hood, D. W.: Carbon Dioxide in the Pacific Ocean and Bering Sea: Upwelling and Mixing, *J. Geophys. Res.*, 76, PP. 745–752, doi:10.1029/JC076i003p00745, 1971.
- Kondo, F. and Tsukamoto, O.: Air-sea CO₂ flux by eddy covariance technique in the equatorial Indian Ocean, *J. Oceanogr.*, 63, 449–456, 2007.
- Largier, J. L., Lawrence, C. A., Roughan, M., Kaplan, D. M., Dever, E. P., Dorman, C. E., Kudela, R. M., Bollens, S. M., Wilkerson, F. P., and Dugdale, R. C.: WEST: A northern California study of the role of wind-driven transport in the productivity of coastal plankton communities, *Deep-Sea Res. Pt. II*, 53, 2833–2849, 2006.
- Lendt, R., Thomas, H., Hupe, A., and Ittekkot, V.: Response of the near-surface carbonate system of the northwestern Arabian Sea to the southwest monsoon and related biological forcing, *J. Geophys. Res.*, 108, 3222, doi:10.1029/2000JC000771, 2003.
- Lentz, S. J.: The surface boundary layer in coastal upwelling regions, *J. Phys. Oceanogr.*, 22, 1517–1539, 1992.
- Nightingale, P. D., Malin, G., Law, C. S., Watson, A. J., Liss, P. S., Liddicoat, M. I., Boutin, J., and Upstill-Goddard, R. C.: In situ evaluation of air-sea gas exchange parameterizations using novel conservative and volatile tracers, *Global Biogeochem. Cy.*, 14, 373–387, doi:10.1029/1999GB900091, 2000.
- Papale, D., Reichstein, M., Aubinet, M., Canfora, E., Bernhofer, C., Kutsch, W., Longdoz, B., Rambal, S., Valentini, R., Vesala, T., and Yakir, D.: Towards a standardized processing of Net Ecosystem Exchange measured with eddy covariance technique: algorithms and uncertainty estimation, *Biogeosciences*, 3, 571–583, doi:10.5194/bg-3-571-2006, 2006.

- Prytherch, J., Yelland, M. J., Pascal, R. W., Moat, B. I., Skjelvan, I., and Neill, C. C.: Direct measurements of the CO₂ flux over the ocean: Development of a novel method, *Geophys. Res. Lett.*, 37, L03607, doi:10.1029/2009GL041482, 2010.
- Sabine, C. L., Feely, R. A., Gruber, N., Key, R. M., Lee, K., Bullister, J. L., Wanninkhof, R., Wong, C. S., Wallace, D. W. R., Tilbrook, B., Millero, F. J., Peng, T.-H., Kozyr, A., Ono, T., and Rios, A. F.: The Oceanic Sink for Anthropogenic CO₂, *Science*, 305, 367–371, doi:10.1126/science.1097403, 2004.
- Sachs, L.: *Angewandte Statistik: Anwendung Statistischer Methoden*, Springer, Berlin, 1996.
- Sarmiento, J. L. and Gruber, N.: *Ocean Biogeochemical Dynamics*, Princeton University Press, Princeton, 2006.
- Schuepp, P. H., Leclerc, M. Y., MacPherson, J. I., and Desjardins, R. L.: Footprint prediction of scalar fluxes from analytical solutions of the diffusion equation, *Bound-Lay. Meteorol.*, 50, 355–373, 1990.
- Simpson, J. J. and Zirino, A.: Biological control of pH in the Peruvian coastal upwelling area, *Deep-Sea Res.*, 27, 733–743, 1980.
- Sweeney, C., Gloor, E., Jacobson, A. R., Key, R. M., McKinley, G., Sarmiento, J. L., and Wanninkhof, R.: Constraining global air–sea gas exchange for CO₂ with recent bomb ¹⁴C measurements, *Global Biogeochem. Cy.*, 21, GB2015, doi:10.1029/2006GB002784, 2007.
- Takahashi, T., Sutherland, S. C., Wanninkhof, R., Sweeney, C., Feely, R. A., Chipman, D. W., Hales, B., Friederich, G., Chavez, F., Sabine, C., Watson, A., Bakker, D. C. E., Schuster, U., Metzl, N., Yoshikawa-Inoue, H., Ishii, M., Midorikawa, T., Nojiri, Y., Körtzinger, A., Steinhoff, T., Hoppema, M., Olafsson, J., Arnarson, T. S., Tilbrook, B., Johannessen, T., Olsen, A., Bellerby, R., Wong, C. S., Delille, B., Bates, N. R., and de Baar, H. J. W.: Climatological mean and decadal change in surface ocean pCO₂, and net sea–air CO₂ flux over the global oceans, *Deep-Sea Res. Pt. II*, 56, 554–577, doi:10.1016/j.dsr2.2008.12.009, 2009.
- Tanner, C. B. and Thurtell, G. W.: Anemoclinometer measurements of Reynolds stress and heat transport in the atmospheric surface layer, ECOM, United States Army Electronics Command, Research and Development Technical Report, ECOM 66-66-G22-F, 1969.
- Torres, R., Turner, D. R., Silva, N., and Rutllant, J.: High short-term variability of CO₂ fluxes during an upwelling event off the Chilean coast at 30° S, *Deep-Sea Res. Pt. I*, 46, 1161–1179, doi:10.1016/S0967-0637(99)00003-5, 1999.
- Vickers, D. and Mahrt, L.: Quality Control and Flux Sampling Problems for Tower and Aircraft Data, *Journal of Atmospheric and Oceanic Technology*, 14, 512–526, doi:10.1175/1520-0426(1997)014<0512:QCAFSP>2.0.CO;2, 1997.
- Wanninkhof, R.: Relationship between wind speed and gas exchange over the ocean, *J. Geophys. Res.*, 97, 7373–7382, doi:10.1029/92JC00188, 1992.
- Wanninkhof, R. and McGillis, W. R.: A cubic relationship between air–sea CO₂ exchange and wind speed, *Geophys. Res. Lett.*, 26, 1889–1892, doi:10.1029/1999GL900363, 1999.
- Webb, E. K., Pearman, G. I., and Leuning, R.: Correction of flux measurements for density effects due to heat and water vapour transfer, *Quart. J. Roy. Meteorol. Soc.*, 106, 85–100, doi:10.1002/qj.49710644707, 1980.
- Weiss, R. F.: Carbon dioxide in water and seawater: the solubility of a non-ideal gas, *Mar. Chem.*, 2, 203–215, doi:10.1016/0304-4203(74)90015-2, 1974.
- Wilkerson, F. P., Lassiter, A. M., Dugdale, R. C., Marchi, A., and Hogue, V. E.: The phytoplankton bloom response to wind events and upwelled nutrients during the CoOP WEST study, *Deep-Sea Res. Pt. II*, 53, 3023–3048, 2006.
- Zhang, J., Lee, X., Song, G., and Han, S.: Pressure correction to the long-term measurement of carbon dioxide flux, *Agr. Forest Meteorol.*, 151, 70–77, doi:10.1016/j.agrformet.2010.09.004, 2011.